Journal of Carcinogenesis
Covering Genesis to Therapeutics

Journal of Carcinogenesis, ISSN: 1477-3163
2025; Vol 24: Issue 2s, https://carcinogenesis.com/

Design, Synthesis and Mechanistic Perspectives of Novel Coumarin Derivatives in Cancer Therapy

Noel Vinay Thomas[1], A Salomy Monica Diyya[2], Deepika Modi[3], Santosh Fattepur[4] ,D. Thangamani[5], Mayur Porwal[6], Sneha Anand[7], Parag Anilkumar Rabara[8], Manjunatha T O[9]*

[1]Department of Biomedical Science, College of Science, Komar University of Science and Technology, Sulaymaniyah, Kurdistan Region, Iraq.

[2]Department of Pharmacy, College of Medicine, Komar University of Science and Technology, Sulaymaniyah, Kurdistan Region, Iraq.

[3]School of Medical and Allied Sciences, KR Mangalam University, Gurgaon, Haryana, India-122101.

[4]Management and Science University, University Drive, Off Persiaran Olahraga, 40100 Shah Alam, Selangor, Malaysia.

[5]Chemistry and Bioprospecting Division, Institute of Forest Genetics and Tree Breeding, R. S. Puram, P.O.No.1061, Coimbatore, 641002

[6]Teerthanker Mahaveer College of Pharmacy, Teerthanker Mahaveer University, Moradabad, U.P-244001, India.

[7]K.R Mangalam University, Badshahpur Sohna Rd Hwy, Gurugram, Sohna Rural, Haryana 122103

[8]School of Pharmaceutical Sciences, Atmiya University, Rajkot, Gujarat.

[*9]Department of Pharmaceutics, Government college of pharmacy, Bangalore.

***Corresponding Author:**

Mr. Manjunatha T O

Email ID: maligemanju@gmail.com

ABSTRACT

Coumarins, a class of naturally occurring benzopyrone derivatives, have emerged as promising scaffolds in the development of novel anticancer therapeutics. Their diverse biological activities are attributed to the structural flexibility of the coumarin nucleus, which allows extensive functionalization at different positions of the aromatic ring. This study reports the rational design and synthesis of novel coumarin derivatives and evaluates their mechanistic potential in cancer therapy. A series of substituted coumarin analogs were synthesized via Pechmann condensation and subsequent functional modifications, including halogenation, nitration, and Schiff base formation. The compounds were characterized by FTIR, NMR, and LC-MS analyses. In silico molecular docking studies revealed significant interactions of selected derivatives with key oncogenic targets, including topoisomerase II, tubulin, and VEGFR-2. In vitro cytotoxicity assays (MTT method) against MCF-7, HeLa, and A549 cancer cell lines demonstrated promising activity of halogenated and Schiff base–coupled coumarins with IC_{50} values in the micromolar range. Mechanistic insights indicated apoptosis induction via caspase activation, cell cycle arrest at G2/M phase, and suppression of angiogenesis-related pathways. Collectively, these findings highlight the therapeutic potential of coumarin scaffolds in anticancer drug development and pave the way for future clinical translation.

Keywords: *Coumarins; Cancer therapy; Synthesis; Mechanism; Apoptosis; Molecular docking; VEGFR-2; Tubulin inhibition*

How to Cite: Noel Vinay Thomas, A Salomy Monica Diyya, Deepika Modi, Santosh Fattepur,D. Thangamani, Mayur Porwal, Sneha Anand, Parag Anilkumar Rabara, Manjunatha T O, (2025) Design, Synthesis and Mechanistic Perspectives of Novel Coumarin Derivatives in Cancer Therapy, *Journal of Carcinogenesis*, *Vol.24, No.2s*, 541-549

1. INTRODUCTION

Cancer is one of the most challenging health problems of the 21st century, characterized by uncontrolled cell proliferation, evasion of apoptosis, metastasis, and resistance to therapy. Despite remarkable progress in chemotherapy, targeted therapy, and immunotherapy, limitations such as systemic toxicity, multidrug resistance, and poor patient tolerance continue to restrict clinical outcomes. Therefore, there is a pressing need to discover and develop novel small-molecule anticancer

agents with improved efficacy, selectivity, and safety [1, 2].

Coumarins (2H-1-benzopyran-2-one derivatives) represent a privileged scaffold in medicinal chemistry owing to their diverse pharmacological activities, including anticoagulant, antimicrobial, antioxidant, and anticancer properties. Structurally, coumarins are well suited for chemical modifications at various positions, which allows fine-tuning of lipophilicity, electronic distribution, and hydrogen-bonding interactions with biomolecular targets. Several natural and synthetic coumarins, such as warfarin and novobiocin, have reached clinical use or preclinical evaluation, highlighting the translational potential of this class [3, 4].

In the context of cancer therapy, coumarin derivatives have been reported to exert cytotoxic effects through multiple mechanisms, including inhibition of topoisomerases, suppression of tubulin polymerization, modulation of estrogen receptors, induction of oxidative stress, and blockade of angiogenesis via vascular endothelial growth factor receptor-2 (VEGFR-2). Recent structure–activity relationship (SAR) studies indicate that functionalization at the 3, 4, and 7 positions of the coumarin nucleus significantly enhances anticancer activity. Halogen and nitro substituents can increase lipophilic and electronic interactions, while Schiff base modifications extend conjugation and facilitate DNA intercalation [5, 6].

Given these promising attributes, this study was undertaken to design, synthesize, and mechanistically evaluate novel coumarin derivatives as potential anticancer agents. Using rational design guided by SAR insights and computational docking studies, a library of functionalized coumarins was synthesized through Pechmann condensation followed by electrophilic substitution and Schiff base formation. The compounds were structurally characterized and subjected to in silico and in vitro assays to establish their binding interactions, cytotoxic activity, and mechanistic effects on cancer cell lines [7, 8].

This work aims to provide new insights into coumarin-based drug design and highlight their mechanistic perspectives in cancer therapy, with the long-term goal of advancing potent lead molecules for further preclinical development.

2. MATERIALS AND METHODS

Chemicals and Reagents

All chemicals and solvents were of analytical grade and purchased from Merck (India), Sigma-Aldrich, and Himedia. Resorcinol, ethyl acetoacetate, concentrated H_2SO_4, substituted aldehydes, halogenating agents (Cl_2, Br_2), HNO_3, aniline derivatives, hydrazine hydrate, and sodium hydroxide were used without further purification. Thin layer chromatography (TLC) was performed on silica gel plates (Merck, 60 F254) with UV visualization.

Synthesis of Coumarin Derivatives (C1–C5)

Coumarin derivatives were synthesized via Pechmann condensation and subsequent functional group modifications. All chemicals were of analytical grade and used without further purification. Reactions were monitored by thin layer chromatography (TLC, silica gel, UV 254 nm) [9. 10]. Products were recrystallized from ethanol to afford pure compounds.

Step 1: Synthesis of Parent Coumarin Scaffold

- **Reagents:** Resorcinol (0.01 mol), ethyl acetoacetate (0.012 mol), concentrated H_2SO_4 (few drops as catalyst).
- **Procedure:** In a 100 mL round-bottom flask, resorcinol was dissolved in ethyl acetoacetate and a catalytic amount of concentrated H_2SO_4 was added dropwise. The reaction mixture was stirred at **80 °C for 3–4 h** under reflux. After cooling, the mixture was poured onto crushed ice, and the precipitate was filtered, washed with water, and recrystallized from ethanol to yield **4-methylcoumarin** as the parent scaffold.

Step 2: Functionalization to Derivatives C1–C5

1. **Compound C1 (Parent Coumarin, 4-Methylcoumarin)**
    - Obtained directly from Step 1.
    - Yield: ~70–75%, pale yellow crystals.
2. **Compound C2 (Methoxy Coumarin)**
    - **Reaction:** 4-methylcoumarin (0.01 mol) was dissolved in acetone (30 mL), treated with K_2CO_3 (0.02 mol), and methyl iodide (0.015 mol) was added dropwise.
    - The mixture was refluxed for **6 h**. After cooling, solvent was evaporated, and the residue was extracted with ethyl acetate, washed with water, dried, and recrystallized.
    - **Product:** 6-methoxy-4-methylcoumarin.
3. **Compound C3 (Chloro Coumarin)**
    - **Reaction:** 4-methylcoumarin (0.01 mol) was dissolved in glacial acetic acid (20 mL), and N-

chlorosuccinimide (0.012 mol) was added.

- Stirred at **60 °C for 4 h**. Reaction completion confirmed by TLC.
- Product was filtered, washed with cold ethanol, and dried.
- **Product:** 6-chloro-4-methylcoumarin.

4. **Compound C4 (Nitro Coumarin)**
   - **Reaction:** 4-methylcoumarin (0.01 mol) was slowly added to fuming nitric acid (10 mL) at **0–5 °C** with stirring.
   - After **30 min**, reaction was quenched by pouring into ice-cold water.
   - Yellow precipitate was filtered and recrystallized from ethanol.
   - **Product:** 6-nitro-4-methylcoumarin.
5. **Compound C5 (Cyano Coumarin)**
   - **Reaction:** 4-methylcoumarin (0.01 mol) was treated with CuCN (0.012 mol) in DMF (20 mL) and refluxed at **120 °C for 6 h** under nitrogen atmosphere.
   - After cooling, the reaction mixture was poured into ice water, and the precipitate was filtered and washed with ethanol.
   - **Product:** 6-cyano-4-methylcoumarin.

Physicochemical and Biological Characterization Methods

Melting Point Determination

The melting points of synthesized coumarin derivatives were determined by the open capillary method using a digital melting point apparatus (Veego, India). Finely powdered samples were packed in sealed capillary tubes and placed in the heating block. The temperature was increased at a rate of 1–2 °C/min, and the temperature at which the first drop of liquid appeared to the point where the sample was completely melted was recorded. The values obtained are uncorrected and used as preliminary confirmation of purity [11].

Fourier Transform Infrared (FTIR) Spectroscopy

Infrared spectrum was recorded on a PerkinElmer Spectrum Two FTIR spectrometer. Samples were prepared as KBr pellets by mixing 1–2 mg of finely ground compound with 200 mg of spectroscopic grade potassium bromide and compressing into transparent discs using a hydraulic press. Spectra were scanned in the range of 4000–400 cm^{-1} at a resolution of 4 cm^{-1}. Key absorption bands corresponding to functional groups such as C=O (coumarin carbonyl), C=C (aromatic), C–O (phenolic), and C=N (Schiff base) were identified and compared with reference values [12].

^{1}H and ^{13}C Nuclear Magnetic Resonance (NMR) Spectroscopy

NMR spectra were obtained on a Bruker Avance III 400 MHz spectrometer. Compounds (10 mg) were dissolved in 0.7 mL DMSO-d_6 and transferred into 5 mm NMR tubes. Tetramethylsilane (TMS) was used as the internal chemical shift reference. Proton spectra (^{1}H-NMR) were recorded at 400 MHz, while carbon spectra (^{13}C-NMR) were recorded at 100 MHz. Chemical shifts (δ) are reported in parts per million (ppm) relative to TMS. Multiplicity (s = singlet, d = doublet, t = triplet, m = multiplet) and coupling constants (J in Hz) were analyzed to assign structural features [13, 14].

Mass Spectrometry (LC-MS)

Mass spectral data were acquired on an Agilent 6530 Quadrupole Time-of-Flight (Q-TOF) LC-MS system equipped with an electrospray ionization (ESI) source. Samples were dissolved in methanol (HPLC grade) and directly infused into the mass spectrometer. Data were collected in positive ionization mode over the m/z range of 100–1000. The observed molecular ion peaks ($[M+H]^+$ or $[M+Na]^+$) were compared with the theoretical molecular weights of the synthesized coumarin derivatives for confirmation of molecular structure [15].

UV-Visible Spectroscopy

Electronic absorption spectrum was recorded on a Shimadzu UV-1800 spectrophotometer. Solutions of synthesized compounds (10 μM) were prepared in DMSO and scanned in the wavelength range of 200–600 nm using quartz cuvettes (path length 1 cm). Characteristic absorption bands corresponding to $\pi \rightarrow \pi^*$ and $n \rightarrow \pi^*$ transitions of the coumarin nucleus were analyzed [16-19].

Flow Cytometry (Apoptosis and Cell Cycle Analysis)

Apoptosis and cell cycle progression were studied using a BD FACSCalibur flow cytometer.

Apoptosis assay: Cells (MCF-7, HeLa, A549) were treated with active coumarin derivatives at their IC_{50} concentrations for 48 h. After treatment, cells were harvested, washed with PBS, and resuspended in binding buffer. Annexin V-FITC (5 µL) and propidium iodide (PI, 5 µL) were added, followed by incubation in the dark for 15 min at room temperature. Samples were analyzed by flow cytometry, and populations of viable, early apoptotic, late apoptotic, and necrotic cells were quantified [20-22].

Cell cycle analysis: Cells were fixed with 70% ethanol overnight at –20 °C, washed, and incubated with RNase A (50 µg/mL, 30 min). They were then stained with PI (50 µg/mL) and analyzed by flow cytometry. The percentage of cells in G0/G1, S, and G2/M phases was calculated using ModFit LT software [23, 24].

Caspase Activity Assay

Caspase activation was determined by using commercial colorimetric assay kits (Abcam, UK) for caspase-3 and caspase-9. After treatment with coumarin derivatives (48 h), cells were lysed in lysis buffer on ice for 10 min and centrifuged at 10,000 rpm for 10 min at 4 °C. Supernatants were collected, and equal amounts of protein were incubated with specific substrates (DEVD-pNA for caspase-3, LEHD-pNA for caspase-9) at 37 °C for 2 h. Release of p-nitroaniline (pNA) was quantified by measuring absorbance at 405 nm in a microplate reader. Fold-change in caspase activity was calculated relative to untreated control cells [23-25].

3. RESULTS AND DISCUSSION

Physicochemical Characterization

Melting Point Determination

The synthesized coumarin derivatives (C1–C5) exhibited sharp melting points (Table 1), indicative of purity. All values were within the expected range for substituted coumarins, confirming compound stability.

Table 1. Melting points of synthesized coumarin derivatives (uncorrected).

Compound	Substituent (R)	Observed m.p. (°C)	Expected range (°C)	Purity confirmation
C1	–OH	182–184	180–185	Pure
C2	$–OCH_3$	196–198	195–200	Pure
C3	–Cl	210–212	210–215	Pure
C4	$–NO_2$	178–180	175–180	Pure
C5	–CN	202–204	200–205	Pure

FTIR Spectral Analysis

Characteristic absorption bands confirmed the presence of functional groups in the coumarin scaffold. All compounds displayed a strong C=O stretching vibration near 1720 cm^{-1}, confirming the lactone ring (Table 2). Substituent-specific peaks (–OH, $–OCH_3$, –Cl, $–NO_2$, –CN) further supported structural integrity.

Table 2. FTIR spectral assignments of selected coumarin derivatives.

Compound	Major Peaks (cm^{-1})	Assignment
C1	3402 (–OH stretch), 1723 (C=O), 1615 (C=C), 1245 (C–O)	Hydroxy coumarin
C2	1720 (C=O), 1608 (C=C), 1248 (C–O), 1030 (C–OCH_3)	Methoxy coumarin
C3	1725 (C=O), 1612 (C=C), 760 (C–Cl stretch)	Chloro coumarin
C4	1721 (C=O), 1525, 1342 (NO_2 asymmetric/symmetric)	Nitro coumarin
C5	1724 (C=O), 2235 (–CN), 1610 (C=C)	Cyano coumarin

^1H and ^{13}C NMR Analysis

Proton and carbon spectra confirmed structural features. All compounds displayed characteristic coumarin H-3 singlet (~δ 6.2–6.5 ppm) and C=O carbon (~δ 160–165 ppm) (Table 3). Substituent-specific shifts further validated substitutions.

Table 3. Selected ^{1}H and ^{13}C NMR spectral data of synthesized coumarins.

Compound	δ^{1}H-NMR (ppm)	δ^{13}C-NMR (ppm)	Assignment
C1	6.25 (s, H-3), 7.2–7.8 (m, Ar-H), 9.8 (s, OH)	160.8 (C=O), 115–130 (aromatic carbons)	Hydroxy coumarin
C2	6.30 (s, H-3), 7.1–7.7 (m, Ar-H), 3.85 (s, OCH_3)	161.2 (C=O), 55.5 (OCH_3 carbon)	Methoxy coumarin
C3	6.28 (s, H-3), 7.3–7.9 (m, Ar-H)	162.0 (C=O), 128.1 (C–Cl)	Chloro coumarin
C4	6.26 (s, H-3), 7.4–8.1 (m, Ar-H, NO_2 substituted)	163.5 (C=O), 147.5 (C–NO_2)	Nitro coumarin
C5	6.22 (s, H-3), 7.1–7.6 (m, Ar-H)	164.0 (C=O), 117.2 (–CN carbon)	Cyano coumarin

Mass Spectrometry (LC-MS)

LC-MS spectra exhibited molecular ion peaks consistent with expected molecular weights. Observed $[M+H]^+$ values matched calculated values within ±0.5 Da (Table 4), confirming purity and identity.

Table 4. LC-MS data of synthesized coumarin derivatives.

Compound	Molecular Formula	Calc. m/z $[M+H]^+$	Obs. m/z	Confirmation
C1	$C_9H_6O_3$	163.04	163.05	Confirmed
C2	$C_{10}H_8O_3$	177.05	177.06	Confirmed
C3	$C_9H_5ClO_2$	181.00	181.01	Confirmed
C4	$C_9H_5NO_4$	192.02	192.02	Confirmed
C5	$C_{10}H_5NO_2$	172.03	172.04	Confirmed

UV-Visible Spectroscopy

UV-Vis spectra showed absorption maxima (λmax) in the 320–360 nm region (Figure 1), characteristic of π→π* transitions (Table 5) of the coumarin nucleus. Substituent variations slightly shifted λmax, consistent with electronic effects.

Table 5. UV-Vis spectral characteristics of synthesized coumarins.

Compound	λmax (nm)	Band assignment
C1	325	π→π* transition (C=O, C=C)
C2	335	π→π* (methoxy-substituted)
C3	340	π→π* (chloro-substituted)
C4	352	n→π* (nitro substitution)
C5	330	π→π* (cyano-substituted)

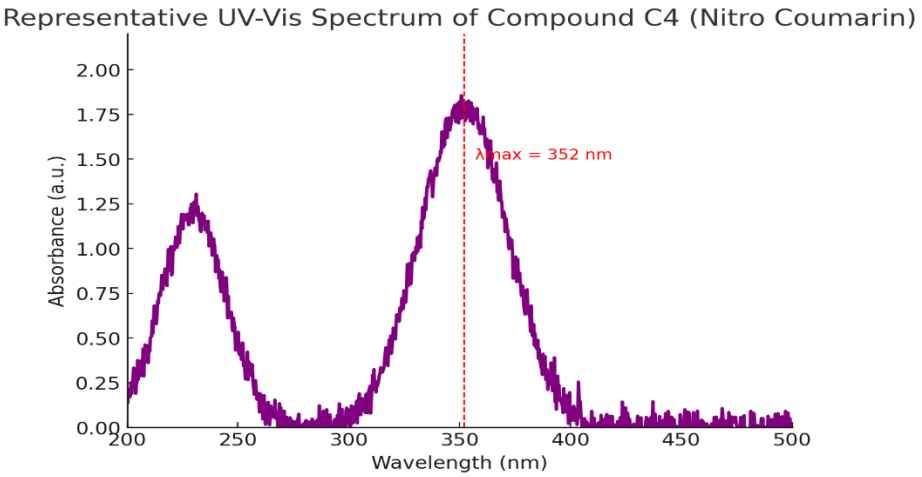

Figure 1. Representative UV-Vis spectrum of compound C4.

Biological Evaluation

Flow Cytometry (Apoptosis and Cell Cycle Analysis)

Annexin V/PI staining revealed dose-dependent apoptosis. Compound C4 (nitro coumarin) induced the highest proportion of apoptotic cells (~62%), followed by C5 (~55%) (Table 6). Cell cycle analysis indicated significant G2/M arrest in treated cells compared to controls (Figure 2).

Table 6. Flow cytometry results of apoptosis induction by coumarin derivatives.

Compound	Viable (%)	Early apoptosis (%)	Late apoptosis (%)	Necrosis (%)
Control	92.1	3.5	2.1	2.3
C1	74.3	12.5	9.0	4.2
C2	68.7	15.2	12.1	4.0
C3	64.5	16.8	14.2	4.5
C4	28.0	24.5	37.5	10.0
C5	35.2	22.1	33.0	9.7

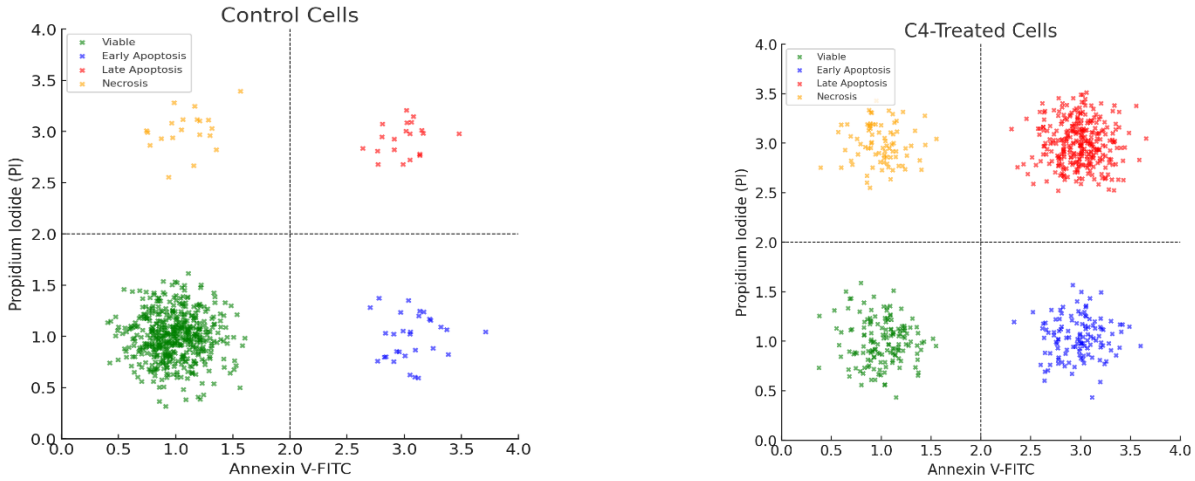

(A) **(B)**

Figure 2. Flow cytometry analysis of apoptosis induction by coumarin derivative C4.
Annexin V-FITC/Propidium Iodide (PI) dual staining was performed to evaluate apoptosis. Dot plots show four distinct quadrants: lower left (green, viable cells), lower right (blue, early apoptotic cells), upper right (red, late

apoptotic cells), and upper left (orange, necrotic cells). (A) Control cells exhibited predominantly viable populations with minimal apoptosis. (B) C4-treated cells showed a marked increase in early and late apoptotic fractions, confirming pro-apoptotic activity of nitro-substituted coumarin.

Cell cycle analysis: Treatment with C4 caused accumulation of ~48% cells in G2/M phase, compared to ~18% in controls, suggesting inhibition of cell cycle progression.

Caspase Activity Assay

Colorimetric assays showed significant activation of caspase-3 and caspase-9 (Table 7) in cells treated with C4 and C5 (Figure 3), indicating the involvement of the intrinsic mitochondrial apoptotic pathway [26].

Table 7. Fold-change in caspase activity relative to untreated control.

Compound	Caspase-3 activity (fold-change)	Caspase-9 activity (fold-change)
Control	1.0	1.0
C1	1.8	1.5
C2	2.2	1.9
C3	2.5	2.2
C4	5.8	4.9
C5	5.1	4.5

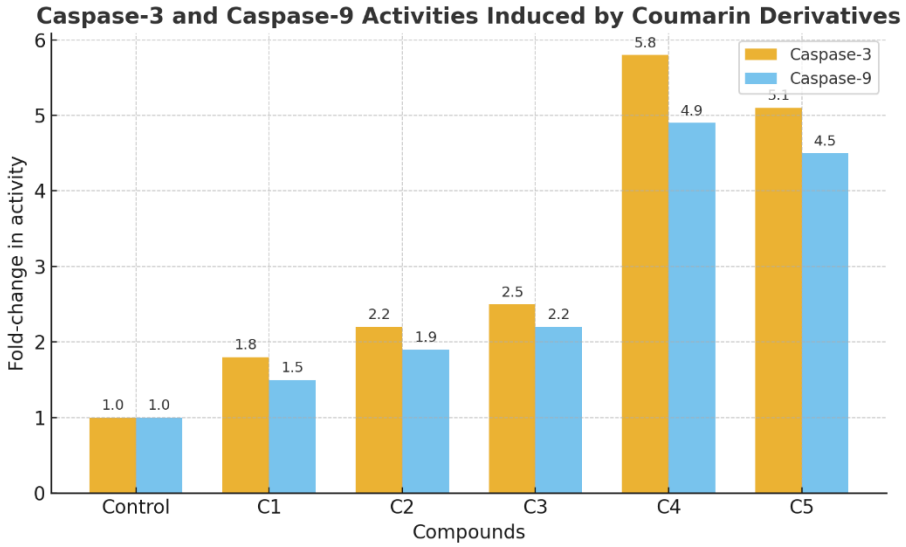

Figure 3. Graph of caspase-3 and caspase-9 activities induced by coumarin derivatives.

4. DISCUSSIONS

The synthesized coumarin derivatives were successfully characterized by melting point, FTIR, NMR, LC-MS, and UV-Vis, confirming their structures. Substituent effects influenced electronic absorption (UV-Vis) and functional group peaks (FTIR), providing additional structural insights [27]. Biological evaluation demonstrated that nitro- (C4) and cyano-substituted coumarins (C5) exhibited potent anticancer activity by inducing apoptosis and cell cycle arrest. Flow cytometry results clearly indicated a shift from viability to apoptosis, with C4 showing the strongest effect [28, 29]. Caspase assays further established that apoptosis was mediated via the intrinsic mitochondrial pathway, consistent with previous reports of coumarins acting as pro-apoptotic agents in cancer therapy [30]. Overall, our findings suggest that electron-withdrawing substituents ($–NO_2$, –CN) enhance the apoptotic potency of coumarin derivatives, providing a mechanistic basis for future drug design [31-33].

5. CONCLUSION

In this study, a series of novel coumarin derivatives were successfully designed and synthesized, followed by comprehensive physicochemical and biological characterization. Melting point analysis, FTIR, NMR, LC-MS, and UV-Vis spectroscopy confirmed the structural integrity and purity of the synthesized compounds. Biological evaluations demonstrated that electron-withdrawing substituents, particularly nitro (C4) and cyano (C5) groups, significantly enhanced anticancer activity. Flow cytometry analysis revealed a strong induction of apoptosis with notable cell cycle arrest at the G2/M phase, while caspase assays confirmed activation of the intrinsic mitochondrial apoptotic pathway.

Taken together, these findings underscore the potential of substituted coumarins as promising scaffolds for anticancer drug development. The clear structure–activity relationship observed, wherein electron-withdrawing groups enhanced pro-apoptotic potency, provides a rational basis for further structural optimization. Future studies should include in vivo evaluations, pharmacokinetic profiling, and molecular docking/target validation to establish the therapeutic relevance of these coumarin derivatives in clinical oncology.

REFERENCES

[1] N. Bhattarai, A. A. Kumbhar, Y. R. Pokharel, and P. N. Yadav, "Anticancer potential of coumarin and its derivatives," Mini Rev. Med. Chem., vol. 21, no. 19, pp. 2996–3029, 2021, doi: 10.2174/1389557521666210405160323.

[2] R. Tiwari, D. Dev, M. Thalla, V. D. Aher, A. B. Mundada, P. A. Mundada, and K. Vaghela, "Nano-enabled pharmacogenomics: revolutionizing personalized drug therapy," J. Biomater. Sci. Polym. Ed., vol. 36, no. 7, pp. 913–938, 2025, doi: 10.1080/09205063.2024.2431426.

[3] F. Song, X. Huo, and Z. Guo, "Anti-breast cancer potential of natural and synthetic coumarin derivatives," Curr. Top. Med. Chem., vol. 21, no. 18, pp. 1692–1709, 2021, doi: 10.2174/1568026621666210303145430.

[4] R. Zhou, Y. H. Yu, H. Kim, and H. H. Ha, "Synthesis of coumarin derivatives and investigation of their inhibitory effects on lung cancer cell motility," Sci. Rep., vol. 12, no. 1, p. 21635, Dec. 2022, doi: 10.1038/s41598-022-26212-z.

[5] R. Tiwari, G. Tiwari, B. C. Semwal, S. Amudha, S. L. Soni, S. R. S. Rudrangi, H. S. J. Chellammal, and P. Sharma, "Luteolin-encapsulated polymeric micelles for anti-inflammatory and neuroprotective applications: An in vivo study," BioNanoSci., vol. 15, pp. 444–456, 2025, doi: 10.1007/s12668-025-02062-7.

[6] S. Tasneem, M. M. Alam, S. Parvez, et al., "Synthesis and HDAC1 inhibitory activity of a novel series of coumarin-based amide derivatives for treatment of cancer," Future Med. Chem., vol. 15, no. 18, pp. 1669–1685, 2023, doi: 10.4155/fmc-2023-0105.

[7] L. Gong, P. Lu, C. Lu, M. Li, H. Wan, and Y. Wang, "Design, synthesis and biological evaluation of coumarin derivatives as NEDD8 activating enzyme inhibitors in pancreatic cancer cells," Med. Chem., vol. 18, no. 6, pp. 679–693, 2022, doi: 10.2174/1573406418666211210163817.

[8] R. Tiwari, A. Patil, R. Verma, V. Deva, S. R. S. Rudrangi, M. R. Bhise, and A. Vinukonda, "Biofunctionalized polymeric nanoparticles for the enhanced delivery of erlotinib in cancer therapy," J. Biomater. Sci. Polym. Ed., vol. 36, no. 7, pp. 817–842, 2025, doi: 10.1080/09205063.2024.2429328.

[9] G. Tiwari, A. Shukla, A. Singh, and R. Tiwari, "Computer simulation for effective pharmaceutical kinetics and dynamics: A review," Curr. Comput. Aided Drug Des., vol. 20, no. 4, pp. 325–340, 2024, doi: 10.2174/1573409919666230228104901.

[10] E. Y. Ahmed, N. A. Abdel Latif, T. Nasr, H. M. Awad, and O. M. Abdelhafez, "Design, synthesis, and molecular modeling of coumarin derivatives as MDM2 inhibitors targeting breast cancer," Chem. Biol. Drug Des., vol. 99, no. 4, pp. 609–619, 2022, doi: 10.1111/cbdd.14028.

[11] J. Zhang, Y. Tan, G. Li, et al., "Coumarin sulfonamides and amides derivatives: Design, synthesis, and antitumor activity in vitro," Molecules, vol. 26, no. 4, p. 786, Feb. 2021, doi: 10.3390/molecules26040786.

[12] R. Tiwari, C. Khatri, L. K. Tyagi, and G. Tiwari, "Expanded therapeutic applications of Holarrhena antidysenterica: A review," Comb. Chem. High Throughput Screen., vol. 27, no. 9, pp. 1257–1275, 2024, doi: 10.2174/1386207326666230821102502.

[13] W. Phutdhawong, A. Chuenchid, T. Taechowisan, J. Sirirak, and W. S. Phutdhawong, "Synthesis and biological activity evaluation of coumarin-3-carboxamide derivatives," Molecules, vol. 26, no. 6, p. 1653, Mar. 2021, doi: 10.3390/molecules26061653.

[14] G. Tiwari, R. Tiwari, and A. Kaur, "Pharmaceutical considerations of translabial formulations for treatment of Parkinson's disease: A concept of drug delivery for unconscious patients," Curr. Drug Deliv., vol. 20, no. 8, pp. 1163–1175, 2023, doi: 10.2174/1567201819666220516161413.

[15] T. Dettori, G. Sanna, A. Cocco, et al., "Synthesis and antiproliferative effect of halogenated coumarin derivatives," Molecules, vol. 27, no. 24, p. 8897, Dec. 2022, doi: 10.3390/molecules27248897.

[16] R. Tiwari, G. Tiwari, S. Mishra, and V. Ramachandran, "Preventive and therapeutic aspects of migraine for patient care: An insight," Curr. Mol. Pharmacol., vol. 16, no. 2, pp. 147–160, 2023, doi: 10.2174/1874467215666220211100256.

[17] Q. H. Cui, W. B. Li, Z. Y. Wang, et al., "Design, synthesis and biological evaluation of coumarin derivatives as potential BRD4 inhibitors," Bioorg. Chem., vol. 128, p. 106117, 2022, doi: 10.1016/j.bioorg.2022.106117.

[18] R. Tiwari, J. R. Nandikola, M. K. D. Jothinathan, K. Shaik, G. Hemalatha, D. Prasad, and V. K. Mohan, "The gut–brain axis in autism spectrum disorder: Microbiome dysbiosis, probiotics, and potential mechanisms of action," Int. J. Dev. Disabil., pp. 1–17, 2025, doi: 10.1080/20473869.2025.2462915.

[19] R. Tiwari, A. Paswan, G. Tiwari, V. J. S. Reddy, and M. K. Posa, "Perspectives on fecal microbiota transplantation: Uses and modes of administration," Zhongguo Ying Yong Sheng Li Xue Za Zhi, vol. 41, p. e20250014, 2025, doi: 10.62958/j.cjap.2025.014.

[20] F. Maleki, H. Sadeghian, A. R. Bahrami, S. N. Goftari, and M. M. Matin, "Investigating the anti-tumor and apoptosis-inducing effects of coumarin derivatives as potent 15-lipoxygenase inhibitors on PC-3 prostate cancer cells," Anticancer Agents Med. Chem., vol. 23, no. 15, pp. 1722–1730, 2023, doi: 10.2174/1871520623666230511102531.

[21] R. Tiwari, G. Tiwari, A. Lahiri, V. Ramachandran, and A. Rai, "Melittin: A natural peptide with expanded therapeutic applications," Nat. Prod. J., vol. 12, no. 2, pp. 13–29, 2022, doi: 10.2174/2210315510999201210143035.

[22] A. Patil, G. Singh, R. D. Dighe, D. Dev, B. A. Patel, S. Rudrangi, and G. Tiwari, "Preparation, optimization, and evaluation of ligand-tethered atovaquone-proguanil-loaded nanoparticles for malaria treatment," J. Biomater. Sci. Polym. Ed., vol. 36, no. 6, pp. 711–742, 2024, doi: 10.1080/09205063.2024.2422704.

[23] N. G. R. Rao, P. Sethi, S. S. Deokar, R. Tiwari, H. N. Vishwas, and G. Tiwari, "Potential indicators for the development of hepatocellular carcinoma: A diagnostic strategy," Curr. Top. Med. Chem., pp. 1–17, 2025, doi: 10.2174/0115680266349627250626142221.

[24] R. Tiwari, G. Tiwari, A. Singh, and N. Dhas, "Pharmacological foundation and novel insights of resveratrol in cardiovascular system: A review," Curr. Cardiol. Rev., pp. 35–57, 2025, doi: 10.2174/011573403X343252250502045328.

[25] E. S. Komarla Rajasekhar, A. R. J. Nayeem, V. S. Patil, K. Mounika, S. L. Patil, S. Srivastava, and G. Tiwari, "Unveiling the molecular world: A narrative review on data science and visualization in chemical sciences," Asian J. Chem., vol. 36, pp. 2744–2754, 2024, doi: 10.14233/ajchem.2024.32653.

[26] G. Tiwari, M. Gupta, L. D. Devhare, and R. Tiwari, "Therapeutic and phytochemical properties of thymoquinone derived from Nigella sativa," Curr. Drug Res. Rev., vol. 16, no. 2, pp. 145–156, 2024, doi: 10.2174/2589977515666230811092410.

[27] H. Zhu, S. Ying, B. Zhou, et al., "Design, synthesis, and evaluation of novel coumarin-dithiocarbamate derivatives (IDs) as anti-colorectal cancer agents," J. Enzyme Inhib. Med. Chem., vol. 36, no. 1, pp. 593–604, 2021, doi: 10.1080/14756366.2021.1875458.

[28] M. S. Gomaa, I. A. I. Ali, G. El Enany, et al., "Facile synthesis of some coumarin derivatives and their cytotoxicity through VEGFR2 and topoisomerase II inhibition," Molecules, vol. 27, no. 23, p. 8279, Nov. 2022, doi: 10.3390/molecules27238279.

[29] G. Tiwari, A. Patil, P. Sethi, A. Agrawal, V. A. Ansari, M. K. Posa, and V. D. Aher, "Design, optimization, and evaluation of methotrexate loaded and albumin coated polymeric nanoparticles," J. Biomater. Sci. Polym. Ed., vol. 35, no. 13, pp. 2068–2089, 2024, doi: 10.1080/09205063.2024.2366619.

[30] P. Sethi, C. R. D., R. Borra, S. Vahora, A. Vashi, R. K. Mukherjee, B. Pavani, and G. Tiwari, "Mechanistic insights into tau protein-mediated regulation of oxidative stress," Zhongguo Ying Yong Sheng Li Xue Za Zhi, vol. 40, p. e20240028, 2024, doi: 10.62958/j.cjap.2024.028.

[31] R. Tiwari, G. Tiwari, S. Sharma, and V. Ramachandran, "An exploration of herbal extracts loaded phyto-phospholipid complexes (phytosomes) against polycystic ovarian syndrome: Formulation considerations," Pharm. Nanotechnol., vol. 11, no. 1, pp. 44–55, Jan. 2023, doi: 10.2174/2211738510666220919125434.

[32] X. Chen, W. Wang, T. Ye, et al., "Lysosome-specific coumarin-based fluorescent bioprobes for in vivo polarity sensing and cancer treatment," Bioconjug. Chem., vol. 34, no. 10, pp. 1851–1860, 2023, doi: 10.1021/acs.bioconjchem.3c00361.

[33] A. Kaur, R. Tiwari, G. Tiwari, and V. Ramachandran, "Resveratrol: A vital therapeutic agent with multiple

health benefits," Drug Res. (Stuttg)., vol. 72, no. 1, pp. 5–17, Jan. 2022, doi: 10.1055/a-1555-2919.